Heat capacity and phase transition of the mixed-valence compound biferrocenium triiodide

ARTICLE *in* JOURNAL OF THE AMERICAN CHEMICAL SOCIETY · JULY 1987

Impact Factor: 12.11 · DOI: 10.1021/ja00248a022

Heat Capacity and Phase Transition of the Mixed-Valence Compound Biferrocenium Triiodide[1]

Michio Sorai,*[2] Akihito Nishimori,[2] David N. Hendrickson,*[3] Teng-Yuan Dong,[3] and Michelle J. Cohn[3]

Contribution from the Chemical Thermodynamics Laboratory, Faculty of Science, Osaka University, Toyonaka, Osaka 560, Japan, and the School of Chemical Sciences, University of Illinois, Urbana, Illinois 61801. *Received October 3, 1986*

Abstract: The results of the measurement of heat capacity at constant pressure, C_p, of the mixed-valence compound biferrocenium triiodide with an adiabatic calorimeter between 14 and 360 K are reported. This compound is known to show a trapped-valence state at low temperature on the ^{57}Fe Mössbauer time scale and a detrapped average valence state at high temperatures. Heat capacity data are presented to show that biferrocenium triiodide exhibits a phase transition in the same temperature region where the valence detrapping occurs on the ^{57}Fe Mössbauer time scale. The present calorimetric measurements indicate a main C_p peak centered at 328 K and two subsidiary small peaks at 312 and 346 K. These three peaks may be attributed to the phase transition arising from different sample histories (mainly different grain sizes of the specimen). The phase transitions are characterized by weak cooperativity; the excess heat capacity due to the phase transition is observed over a wide temperature region from ~220 to ~360 K. The transition entropy was found to be $\Delta S_{trs} = (1.77 \pm 0.06)$ J K^{-1} mol^{-1}. This value is unexpectedly small even if one takes into account only the contribution from the onset of intramolecular electron transfer in the binuclear cations, which amounts to R ln 2 (=5.76 J K^{-1} mol^{-1}), where R is the gas constant. Based on the temperature acquisition of ΔS_{trs}, the average of the potential energy difference between two electron-localized states, [$Fe_A^{II}Fe_B^{III}$] and [$Fe_A^{III}Fe_B^{II}$], was estimated. The result indicates incompleteness of the phase transitions. A qualitative microscopic model for the phase transition is presented. Intermolecular interactions in the stacks of mixed-valence cations are suggested to be important. In order to have a phase transition it is also important to have interactions between a given cation and its neighboring I_3^- anions. In order to examine the role of the I_3^- counteranion, far-infrared and Raman spectra have been recorded in the range below 400 cm^{-1} as a function of temperature. The symmetric stretching mode (ν_1) of the I_3^- anion was observed at 110 cm^{-1} in the Raman spectrum while the deformation (ν_2) and asymmetric stretching (ν_3) modes were observed at 55 and 136 cm^{-1} in the IR spectrum. The observation of such a mutual exclusion of vibrational modes between the IR and Raman experiments suggests that the I_3^- anion in biferrocenium triiodide has nearly a linear symmetrical form, and thus a charge oscillation between two distorted forms I$^-$···I–I and I–I···I$^-$ does not occur in the range 101–340 K. At the very least the distortion of the I_3^- anion in biferrocenium triiodide is not as appreciable as it is in other statically distorted cases. IR and Raman data are also presented for the analogous mixed-valence compound 1′,6′-dichlorobiferrocenium triiodide hemiiodine. In keeping with the X-ray structural results, which show an asymmetric I_3^- anion in this compound, all three I_3^- vibrational modes are seen both in the IR and Raman spectra.

The study of polynuclear mixed-valence complexes in the solid state is providing insight about fundamental factors influencing the rate of electron transfer between metal ions.[4] In particular, the influence of the environment of the electron-transfer rate can be probed with mixed-valence complexes in the condensed phase. This is the case because in the solid state it is possible to obtain detailed structural, spectroscopic, and thermodynamic data. The effects on the rate of intramolecular electron transfer of environmental factors such as the symmetry of the environment and the onset of motion associated with ligands, solvate molecules, and counterions can be studied. In the case of trinuclear mixed-valence iron acetate complexes in the solid state, the onset of motion of a ligand[5,6] or solvate molecule[6-9] has been found to affect the rate of electron transfer. Solid-state ^{2}H NMR data measured for a single-crystal and polycrystalline samples have provided detailed information about the solid-state dynamics.[7-9] It has been found that in several cases the intramolecular electron-transfer process is coupled to a phase transition.[10-12] In the case of these trinuclear mixed-valence iron acetate complexes a detailed theoretical model has been presented to show what types of phase transitions involving an electronic localization–delocalization transformation are possible.[13]

Recent results reported for binuclear mixed-valence biferrocenes also clearly indicate that the nature of the solid-state environment about a mixed-valence cation can dramatically affect the rate of intramolecular electron transfer.[6,14-21] Several important observations have been made on the mixed-valence compounds **1–8** and related complexes. The nature of the I_3^- anion, i.e., whether it is symmetric or asymmetric, and the placement of the I_3^- anion relative to the mixed-valence cation impact on the rate of electron

(1) Contribution No. 106 from the Chemical Thermodynamics Laboratory.
(2) Osaka University.
(3) University of Illinois.
(4) For recent reviews on mixed-valence complexes, see: (a) Day, P. *Int. Rev. Phys. Chem.* **1981**, *1*, 142. (b) *Mixed-Valence Compounds, Theory and Applications in Chemistry, Physics, Geology and Biology*; Brown, D. B., Ed.; Reidel: Boston, 1980. (c) Creutz, C. *Prog. Inorg. Chem.* **1983**, *30*, 1–73. (d) Richardson, D. E; Taube, H. *Coord. Chem. Rev.* **1984**, *60*, 107–129.
(5) (a) Oh, S. M.; Hendrickson, D. N.; Hassett, K. L.; Davis, R. E. *J. Am. Chem. Soc.* **1984**, *106*, 7984. (b) Oh, S. M.; Hendrickson, D. N.; Hassett, K. L.; Davis, R. E. *J. Am. Chem. Soc.* **1985**, *107*, 8009.
(6) Hendrickson, D. N.; Oh, S. M.; Dong, T.-Y.; Kambara, T.; Cohn, M. J.; Moore, M. F. *Comments Inorg. Chem.* **1985**, *4*, 329.
(7) Woehler, S. E.; Wittebort, R. J.; Oh, S. M.; Hendrickson, D. N.; Inniss, D.; Strouse, C. E. *J. Am. Chem. Soc.* **1986**, *108*, 2938.
(8) Woehler, S. E.; Wittebort, R. J.; Oh, S. M.; Kambara, T.; Hendrickson, D. N.; Inniss, D. Strouse, C. E. *J. Am. Chem. Soc.* **1987**, *109*, 1063.
(9) Oh, S. M.; Wilson, S. R.; Hendrickson, D. N.; Woehler, S. E.; Wittebort, R. J.; Inniss, D.; Strouse, C. E. *J. Am. Chem. Soc.* **1987**, *109*, 1073.
(10) Oh, S. M.; Kambara, T.; Hendrickson, D. N.; Sorai, M.; Kaji, K.; Woehler, S. E.; Wittebort, R. J. *J. Am. Chem. Soc.* **1985**, *107*, 5541.
(11) Sorai, M.; Kaji, K.; Hendrickson, D. N.; Oh, S. M. *J. Am. Chem. Soc.* **1986**, *108*, 702.
(12) Sorai, M.; Shiomi, Y.; Hendrickson, D. N.; Oh, S. M.; Kambara, T. *Inorg. Chem.* **1987**, *26*, 223.
(13) Kambara, T.; Hendrickson, D. N.; Sorai, M.; Oh, S. M. *J. Chem. Phys.* **1986**, *85*, 2895.
(14) Dong, T.-Y.; Hendrickson, D. N.; Pierpont, C. G.; Moore, M. F. *J. Am. Chem. Soc.* **1986**, *108*, 963.
(15) Dong, T.-Y.; Hendrickson, D. N.; Iwai, K.; Cohn, M. J.; Rheingold, A. L.; Sano, H.; Motoyama, I.; Nakashima, S. *J. Am. Chem. Soc.* **1985**, *107*, 7996.
(16) Cohn, M. J.; Dong, T.-Y.; Hendrickson, D. N.; Geib, S. J.; Rheingold, A. L. *J. Chem. Soc., Chem. Commun.* **1985**, 1095.
(17) Dong, T.-Y.; Kambara, T.; Hendrickson, D. N. *J. Am. Chem. Soc.* **1986**, *108*, 4423.
(18) Dong, T.-Y.; Kambara, T.; Hendrickson, D. N. *J. Am. Chem. Soc.* **1986**, *108*, 5857.
(19) Dong, T.-Y.; Cohn, M. J.; Hendrickson, D. N.; Pierpont, C. G. *J. Am. Chem. Soc.* **1985**, *107*, 4777.
(20) Moore, M. F.; Wilson, S. R.; Cohn, M. J.; Dong, T.-Y.; Mueller-Westerhoff, U. T.; Hendrickson, D. N. *Inorg. Chem.* **1985**, *24*, 4559.
(21) Geib, S. J.; Rheingold, A. L.; Dong, T.-Y.; Hendrickson, D. N. *J. Organomet. Chem.* **1986**, *312*, 241.

0002-7863/87/1509-4266$01.50/0

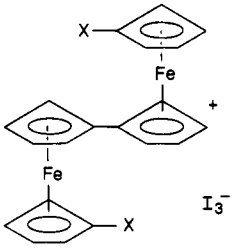

1, X = H 5, X = CH_2CH_3
2, X = Cl 6, X = $CH_2CH_2CH_3$
3, X = I 7, X = $CH_2CH_2CH_2CH_3$
4, X = Br 8, X = CH_2 

transfer. Compound **2** crystallizes with 0.5 mol of I_2, and the X-ray structure[14] shows that not only is the I_3^- anion asymmetric but the I_3^- counterion sits closer to one-half of the cation, the iron(III) metallocene moiety, than the iron(II) moiety. As a result, **2** is localized on the Mössbauer time scale even at 340 K. The double-well potential energy surface for the ground state of the mixed-valence cation in **2** is asymmetric due to the asymmetric environment about the cation. Intramolecular electron transfer is slow (rate < $10^7 s^{-1}$ at 340 K). The localization of other binuclear mixed-valence biferrocene[21] and ferrocenophane[20] complexes has also been shown to occur as a result of the placement of the anion relative to the mixed-valence cation.

The X-ray structure of **3** shows that the two metallocene moieties of the cation are crystallographically equivalent.[14] The rate of electron transfer in **3** (and isostructural **4**) exceeds the Mössbauer[14,22,23] (>$10^7 s^{-1}$) and EPR[14] (>10^9–$10^{10} s^{-1}$) time scales not only at 300 K but also at 4.2 K, in spite of the fact that IR data[14,24] on **3** and **4** clearly indicate that the mixed-valence cations in these two compounds do have potential energy barriers for electron transfer (tunneling at 4.2 K?). Compounds **1** and **5**–**8** are valence localized at low temperatures, but as well-crystallized salts they interconvert (electron transfer) faster than the Mössbauer time scale at 357,[15,16] 275,[25] 245,[25] 275,[15] and 260 K,[15] respectively.

From the X-ray structures of **1**,[15,16] **2**,[14] **3**,[14] **6**,[26] **7**,[15] and **8**[27] it is known that all of these mixed-valence biferrocene cations have a trans conformation with a planar fulvalenide ligand. Furthermore, there seems to be appreciable intermolecular interactions present in these solids. Compounds **1** and **6**–**8** (also probably **5**) have packing arrangements consisting of segregated stacks of cations and anions. Each cation stack is surrounded by four stacks of anions. There are appreciable cation–cation interactions within a cation stack. In **1** the cation stack develops in a stepwise fashion, and the intrastack cation–cation interaction comes in the form of a cp···cp contact with an interplanar distance of only 3.4 Å.[15,16] Because of the propyl substituents, the cations in **6** slip further apart relative to what is found in **1**; however, there still is a cp···cp contact in **6**. The even bulkier substituents of the cations **7** and **8** lead to an even greater intrastack cation–cation distance. In **7** and **8** there is not a direct cp···cp contact between cations; however, the cation–cation intermolecular interaction is propagated by the substituent X.

The evidence for the presence of phase transitions which affect the rate of intramolecular electron transfer for mixed-valence biferrocenes in the solid state is growing. On the one hand, pronounced sample history dependencies of rates of electron transfer, as detected by ^{57}Fe Mössbauer spectroscopy, have been noted for some of the above compounds.[15] For example, it has been found that a microcrystalline sample of **8** gives a 300 K Mössbauer spectrum which is dominantly that of a valence-localized species (i.e., two doublets). However, a crystalline sample of **8** grown by diffusion gives a 300 K Mössbauer spectrum with one average-valence doublet. Additional evidence for the importance of intermolecular interactions, and therefore potentially phase transitions, is found in the fact that the rate of electron transfer for a particular mixed-valence cation changes dramatically with a change in the anion.[16–18] For example, replacing I_3^- in compound **1** by Br_2I^- to give a compound isostructural with **1** reduces by 150 deg the temperature at which the biferrocenium cation transfers an electron faster than the Mössbauer technique can sense.

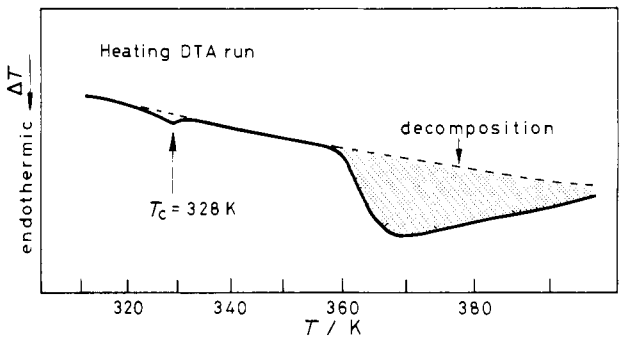

Figure 1. Heating run of DTA for biferrocenium triiodide crystal. Shaded peak corresponds to decomposition of the sample.

In this paper definitive evidence for the presence of a phase transition in biferrocenium triiodide, **1**, is presented. The constant-pressure heat capacity, C_p, of **1** has been measured from 14 to 360 K. It was anticipated that, if there is a phase transition associated with the electron-transfer process in **1**, the phase transition should occur in the range 300–357 K. It is in this temperature range where Mössbauer data have shown[15,16] that **1** converts from valence trapped to valence detrapped.

Experimental Section

Sample Preparation. Samples of biferrocene were prepared according to a literature method.[28] The ~11-g sample of biferrocenium triiodide was prepared in two batches, one ~8 g and the other ~3 g. Both batches were prepared by slowly adding over a period of 3 h a stoichiometric amount of I_2 dissolved in benzene to a stirred benzene solution of biferrocene. The resulting microcrystalline sample was washed with benzene and dried in a desiccator. Anal. Calcd for biferrocenium triiodide ($C_{20}H_{18}Fe_2I_3$): C, 32.00; H, 2.42; Fe, 14.88; I, 50.71. Found (two preparations): C, 32.79, 32.50; H, 2.56, 2.42; Fe, 14.77, 14.63; I, 50.46, 50.47.

Thermal Analysis. Preliminary observation of the thermal properties of the biferrocenium triiodide specimen for heat capacity measurements was made with a home-built differential thermal analysis (DTA) apparatus at the Chemical Thermodynamics Laboratory of Osaka University. The dependence of the phase-transition behavior upon the sample history was examined with a Perkin-Elmer Model DSC 7 differential scanning calorimeter at the School of Chemical Sciences of the University of Illinois. The mass of sample used for a probe was ~300 mg for DTA and ~6–17 mg for DSC.

Heat Capacity Measurements. Heat capacities were measured with an adiabatic calorimeter[29] from 14 to 360 K. A calorimeter cell[30] made of gold and platinum contained 10.9428 g (or 0.014 575 42 mol) of polycrystalline biferrocenium triiodide. A small amount of helium gas was sealed in the cell to aid the heat transfer.

Infrared Absorption Spectra. Spectra in the range 4000–400 cm^{-1} were recorded for Nujol mulls with an infrared spectrophotometer (Japan Spectroscopic Co., Ltd., Model DS-402G) and far-infrared spectra in the range 400–30 cm^{-1} with a far-infrared spectrophotometer (Hitachi, Ltd., Model FIS-3).

Raman Spectra. Multitemperature Raman spectra in the range 300–40 cm^{-1} were recorded for powdered crystals of biferrocenium tri-

(22) Morrison, W. H., Jr.; Hendrickson, D. N. *Inorg. Chem.* **1975**, *14*, 2331.
(23) Motoyama, I.; Suto, K.; Katada, M.; Sano, H. *Chem. Lett.* **1983**, 1215.
(24) Kramer, J. A.; Hendrickson, D. N. *Inorg. Chem.* **1980**, *19*, 3330.
(25) Iijima, S.; Saida, R.; Motoyama, I.; Sano, H. *Bull. Chem. Soc. Jpn.* **1981**, *54*, 1375.
(26) Konno, M.; Hyodo, S.; Iijima, S. *Bull. Chem. Soc. Jpn.* **1982**, *55*, 2327.
(27) Dong, T.-Y.; Hendrickson, D. N.; Pierpont, C. G., unpublished results.
(28) Rausch, M. D. *J. Org. Chem.* **1961**, *26*, 1802.
(29) Sorai, M.; Kaji, K., construction of an adiabatic calorimeter capable of measuring heat capacities between 12 and 530 K (unpublished).
(30) Tsuji, K.; Sorai, M.; Suga, H.; Seki, S. *Mol. Cryst. Liq. Cryst.* **1979**, *55*, 71.

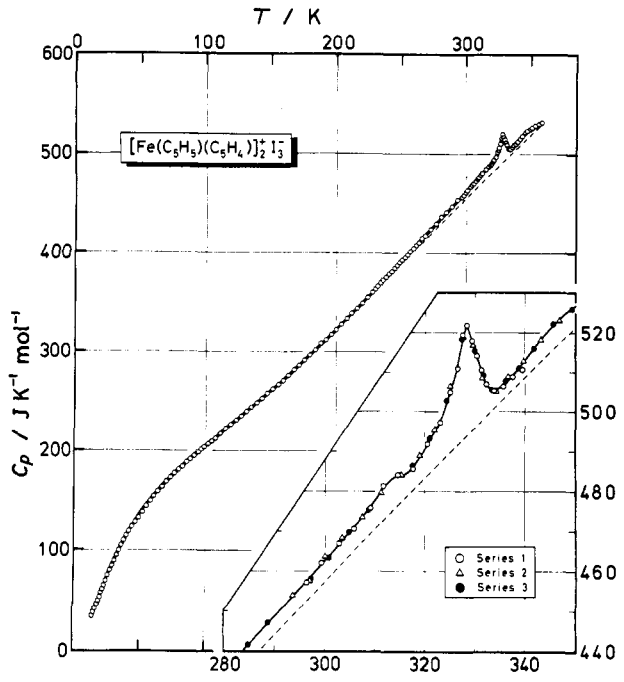

Figure 2. Molar heat capacity of biferrocenium triiodide. Broken lines indicate the normal heat capacity curve.

iodide with a laser Raman spectrophotometer (Japan Spectroscopic Co., Ltd., Model R-800) using the 632.8-nm line from a He–Ne source for excitation and the 514.5-nm line from an Ar source.

Results and Discussion

Heat Capacity of Biferrocenium Triiodide. The thermal properties of mixed-valence biferrocenium triiodide were preliminarily examined by DTA. Thermograms exhibited a single broad peak at 328 K on the heating run and at 325–326 K on cooling. Therefore, the occurrence of a phase transition in the present sample was established. Figure 1 shows a DTA run which was intended to record the decomposition temperature of the compound. The decomposition process covered a very wide temperature region starting from ~360 K. Although the decomposed products have not been characterized, this decomposition reaction seems to involve mainly the reaction $I_3^- \rightleftharpoons I^- + I_2$. The reason for this conjecture is the fact that the peak at 328 K arising from the phase transition and the broad decomposition peak were reproduced, though incompletely, by repeated cycles of DTA runs between 300 and 400 K. This reproducibility might be possible here as the present DTA probe consisted of a sealed glass tube. From this experiment the highest temperature below which the calorimetric measurements can safely be made without damaging the sample was determined to be ~360 K.

Calorimetric measurements on a 10.9428-g sample of biferrocenium triiodide were made in four series with an adiabatic calorimeter between 14 and 360 K. The results were evaluated in terms of C_p, the molar heat capacity at constant pressure. The experimental data are listed in Table I and plotted in Figure 2. The thermal anomaly detected at 328 K by DTA was observed by the heat capacity measurements as a broad peak centered at the same temperature. As the thermal effect of this phase transition was very small, the C_p measurements were carefully repeated in series 1–3 of Table I. Thermal relaxation time, the time required for thermal equilibration in the specimen after a Joule energy input to the calorimeter cell, was normal even in the vicinity of the phase-transition temperature.

Biferrocenium triiodide can roughly be regarded as consisting of 2 ferrocene molecules and 1.5 I_2 molecules. We then tried to compare the heat capacity of biferrocenium triiodide with the sum of the contributions from these two "components" (eq 1). In the

$$C_p = 2C_p(\text{ferrocene}) + 1.5C_p(I_2) \quad (1)$$

case of ferrocene, two crystal polymorphs exist at low temperatures:[31,32] one is the metastable triclinic ferrocene in which the two cyclopentadienyl rings are mutually rotated by about 9° from the eclipsed orientation,[33] while the other is the stable orthorhombic ferrocene in which the molecules are exactly eclipsed.[34,35] Since

Table I. Molar Heat Capacity of Biferrocenium Triiodide Crystal[a]

T, K	C_p, J K^{-1} mol^{-1}	T, K	C_p, J K^{-1} mol^{-1}	T, K	C_p, J K^{-1} mol^{-1}
		Series 1			
296.264	457.02	320.586	491.90	330.365	514.21
299.281	462.00	323.041	497.17	331.337	510.54
302.795	466.80	324.998	504.91	332.310	507.05
305.789	470.48	326.475	510.86	333.774	505.40
309.104	475.78	327.459	519.36	335.725	506.41
311.709	481.29	328.427	521.73	337.676	508.76
314.680	484.14	329.395	517.89	339.627	510.47
317.632	485.54				
		Series 2			
293.583	453.92	318.864	489.13	336.727	508.95
296.769	457.90	321.986	495.36	339.818	512.75
299.958	463.75	325.094	506.53	343.289	518.22
303.524	468.32	327.607	518.71	347.140	523.28
307.475	473.54	329.534	516.84	350.983	526.59
311.413	479.73	331.466	508.44	354.827	528.98
315.340	484.01	334.214	505.48	358.675	532.52
		Series 3			
14.317	34.188	92.143	194.41	224.500	355.05
15.399	37.747	95.164	198.93	228.544	360.08
16.487	41.720	97.232	201.03	232.592	366.30
17.567	45.434	99.684	203.38	236.645	372.44
18.650	49.016	102.543	206.57	241.119	378.38
19.738	52.761	105.350	209.36	245.318	384.28
20.822	57.166	108.111	212.42	249.380	390.18
21.914	60.944	112.139	217.42	253.435	395.74
23.016	64.319	115.769	221.50	257.482	401.27
24.384	69.095	119.733	225.85	261.521	407.27
25.976	74.528	123.694	230.46	265.553	412.87
27.550	79.625	127.658	234.20	268.699	417.25
29.177	84.306	131.563	239.20	272.734	423.49
30.875	89.319	135.412	243.51	276.761	429.51
32.634	94.597	139.378	247.83	280.783	436.08
34.445	99.897	143.459	252.28	284.797	441.54
36.305	104.89	147.491	257.25	288.800	446.95
38.212	110.10	151.510	261.96	296.769	457.75
40.165	114.82	156.073	266.86	300.756	463.18
42.159	119.09	159.640	270.45	304.753	469.79
44.403	123.71	163.569	275.79	308.756	475.44
46.837	128.13	167.628	281.05	317.513	486.51
49.455	132.75	171.816	285.87	321.035	493.38
52.482	138.32	175.967	291.34	324.152	502.86
55.549	144.29	180.084	296.58	327.250	518.77
58.450	149.55	184.167	301.92	329.761	515.37
61.248	154.07	188.222	308.24	331.696	509.33
64.153	158.89	192.245	311.46	333.633	505.37
67.329	163.60	196.239	316.88	336.149	507.85
70.590	168.85	200.294	321.92	338.854	510.98
73.782	172.94	204.329	327.39	341.936	515.96
76.924	176.76	208.362	333.26	345.780	522.24
80.031	180.68	212.393	339.02	349.615	526.13
83.111	183.40	216.425	343.73	353.445	528.86
86.174	188.45	220.461	349.28	356.465	530.66
89.159	191.21				
		Series 4			
226.584	358.15	243.279	380.87	255.447	398.60
230.632	363.51	247.341	387.22	259.497	404.05
234.686	369.48	251.397	392.79	263.545	410.09
238.983	375.36				

[a] Relative molecular mass = 750.77042.

(31) Ogasahara, K.; Sorai, M.; Suga, H. *Chem. Phys. Lett.* **1979**, *68*, 457.
(32) Ogasahara, K.; Sorai, M.; Suga, H. *Mol. Cryst. Liq. Cryst.* **1981**, *71*, 189.
(33) Seiler, P.; Dunitz, J. D. *Acta Crystallogr., Sect. B: Struct Crystallogr. Cryst. Chem.* **1979**, *B35*, 2020.
(34) Bĕrar, J. F.; Calvarin, G.; Weigel, D.; Chhor, K. Pommier, C. *J. Chem. Phys.* **1980**, *73*, 438.
(35) Seiler, P.; Dunitz, J. D. *Acta Crystallogr., Sect. B: Struct Crystallogr. Cryst. Chem.* **1982**, *B38*, 1741.

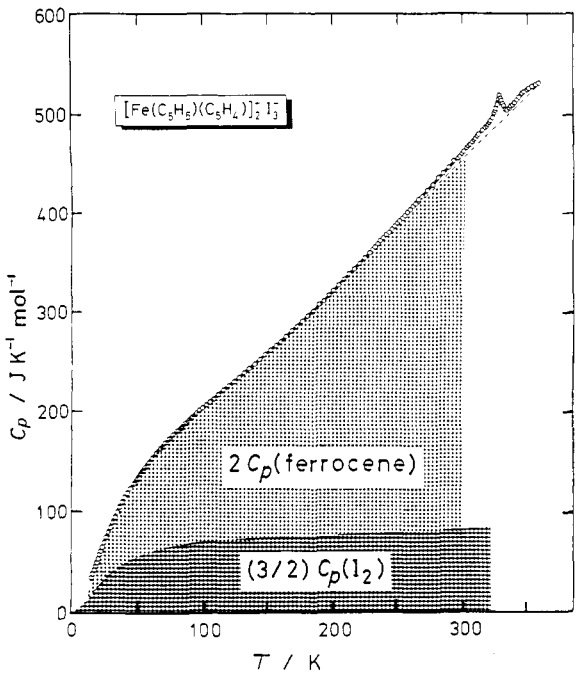

Figure 3. Comparison of the molar heat capacity of biferrocenium triiodide with the sum of the heat capacities of 2 mol of ferrocene[32] and 1.5 mol of iodine.[36] Broken line indicates the normal heat capacity curve to separate the phase transition.

the mixed-valence biferrocenium cation has a trans conformation and the two rings of each $Fe(C_5H_5)(C_5H_4)$ moiety are eclipsed,[15,16] the heat capacity of the orthorhombic ferrocene was used for comparison below ~230 K while for the temperature region above ~230 K the C_p data of monoclinic ferrocene,[32] which is the stable high-temperature phase, were adopted. On the other hand, for the heat capacity of crystalline iodine, we used the data of Shirley and Giauque.[36] As illustrated in Figure 3, agreement between the observed heat capacity, C_p(obsd), and the calculated heat capacity, C_p(calcd), is surprisingly good. For instance, the difference between the two is smaller than 2% of C_p(obsd) in the range 100–260 K. This fact seems to suggest that the chemical bond in the fulvalenide ligand linking the two five-membered rings is weak, and hence the mixed-valence biferrocenium cation behaves as if the cation consists of two independent metallocene moieties and, since the bending vibrational mode of the I_3^- anion is very soft, the thermal properties of the I_3^- ion can be approximated in terms of 1.5 mol of I_2 molecule. In fact, a very low bending frequency, 69 cm^{-1}, has been reported for the CsI_3 crystal[37] in which the distance between two terminal iodine atoms (5.882 Å)[38] of the I_3^- anion at room temperature is nearly equal to the distance (5.8584 Å) found for the I_3^- anion of biferrocenium triiodide.[15,16]

To estimate the excess heat capacities due to the phase transition from the experimental values, a "normal" heat capacity curve was determined by an effective frequency distribution method.[39] Since biferrocenium triiodide consists of 43 atoms, the number of degrees of freedom for molecular vibration is 129. Among them, 24 modes of intramolecular vibration above 800 cm^{-1} (82 degrees of freedom) were assigned on the basis of the present IR spectra. The contributions of these modes to the normal heat capacity were calculated according to the Einstein model. The contributions from the remaining 47 degrees of freedom were included in the effective frequency spectrum. Close inspection of the C_p vs. T curve shown in Figure 2 suggests a crossover of two straight-line behaviors at ~200 K; one is a straight line covering the range ~80 to ~200 K, and the other is a line in the range ~200 to ~310 K. This crossover temperature just corresponds to the temperature at which the plot of the natural logarithm of the ^{57}Fe Mössbauer spectral area vs. temperature for biferrocenium triiodide changes from one straight line to a second straight line.[15] From this coincidence of the crossover temperatures for heat capacity and Mössbauer data it can be deduced that the phase transition arising from the intramolecular electron transfer in the mixed-valence biferrocenium cation probably starts to occur at ~200 K. Therefore, 62 C_p values in the range 14–200 K and the C_p value measured at the highest temperature (358.675 K, the last point in series 2 in Table I) were used for determination of a normal heat capacity curve. The highest temperature point was included in the calculation to avoid trivial deviation of the otherwise estimated normal heat capacity curves from the observed C_p value at the highest temperature. The "best" three effective frequency distributions below 700 cm^{-1} were determined by the least-squares method (labeled A, B, and C in Table II). The normal heat capacity at rounded temperatures and the highest temperature studied here are listed in Table II. The present methods reproduce the experimental C_p values below 200 K within a root-squares deviation of ±0.404, ±0.518, and ±0.566 J K^{-1} mol^{-1} for the three frequency spectra A, B, and C, respectively. Broken lines shown in Figures 2 and 3 are the normal heat capacity derived from the spectrum A.

Table II. Normal Heat Capacity and the Enthalpy and Entropy of Transition for Biferrocenium Triiodide Crystal

T,[a] K	C_p(normal) at effective frequency spectrum, J K^{-1} mol^{-1} A[b]	B[c]	C[d]	C_p(obsd), J K^{-1} mol^{-1}
	Fitting Region			
20	54.26	54.68	54.74	53.83
40	113.61	113.33	113.15	114.42
60	152.46	152.56	152.18	152.05
80	180.61	180.69	180.74	180.64
100	203.99	203.92	204.20	203.73
120	225.90	225.83	226.02	226.16
140	248.17	248.15	248.14	248.51
160	271.59	271.63	271.44	270.94
180	296.33	296.40	296.14	296.47
200	322.23	322.31	322.07	321.56
358.675	532.10	531.85	533.01	532.52
	Interpolated Region			
210	335.53	335.59	355.40	335.60
220	348.99	349.04	348.91	348.64
230	362.58	362.62	362.55	362.47
240	376.24	376.26	376.28	376.80
250	389.94	389.95	390.05	390.98
260	403.64	403.62	403.82	404.85
270	417.30	417.25	417.55	419.26
280	430.88	430.81	431.21	434.80
290	444.35	444.26	444.75	448.70
300	457.68	457.57	458.17	463.72
310	470.86	470.72	471.42	477.31
320	483.85	483.69	484.49	490.96
330	496.65	496.46	497.35	514.91
340	509.23	509.02	510.00	513.03
350	521.58	521.35	522.42	526.26
ΔS_{trs},[e] J K^{-1} mol^{-1}	1.779	1.821	1.697	
ΔH_{trs},[f] J mol^{-1}	552.2	565.9	497.0	

[a] Temperature region for fitting is 14–200 K and 358.675 K. [b] Root mean square deviation of C_p is ±0.404. [c] Root mean square deviation of C_p is ±0.518. [d] Root mean square deviation of C_p is ±0.566. [e] ΔS_{trs}(average) = (1.77 ± 0.06) J K^{-1} mol^{-1}. [f] ΔH_{trs}(average) = (538 ± 37) J mol^{-1}.

Excess Heat Capacity due to Phase Transition. The difference between the observed and normal heat capacities corresponds to the excess heat capacity, ΔC_p, due to the phase transition. In Figure 4, ΔC_p is plotted as a function of temperature. The enthalpy (ΔH_{trs}) and entropy (ΔS_{trs}) arising from the phase transition were determined by integration of ΔC_p with respect to T and ln T, respectively. The average values of the transition enthalpies and entropies derived from different normal heat capacities are

(36) Shirley, D. A.; Giauque, W. F. *J Am. Chem. Soc.* **1959**, *81*, 4778.
(37) Maki, A. G.; Forneris, R. *Spectrochim. Acta, Part A* **1967**, *23A*, 867.
(38) Runsink, J.; Swen-Walstra, S.; Migchelsen, T. *Acta Crystallogr., Sect. B: Struct Crystallogr. Cryst. Chem.* **1972**, *B28*, 1331.
(39) Sorai, M.; Seki, S. *J. Phys. Soc. Jpn.* **1972**, *32*, 382.

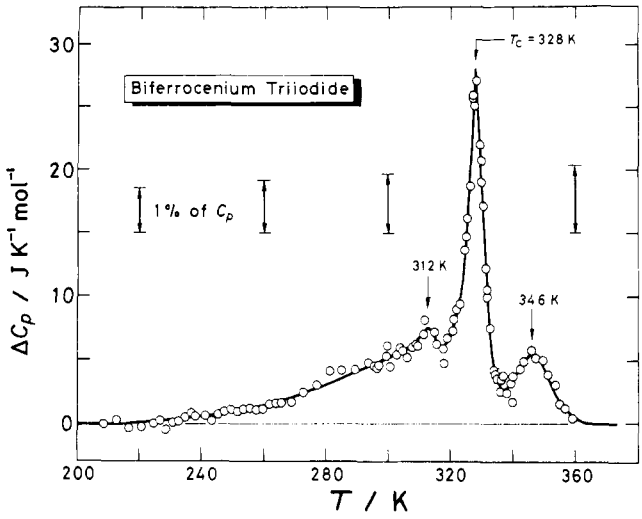

Figure 4. Excess heat capacity, ΔC_p, due to the phase transition of *biferrocenium triiodide.*

ΔH_{trs} = (538 ± 37) J mol^{-1} and ΔS_{trs} = (1.77 ± 0.06) J K^{-1} mol^{-1} (see Table II).

In the ΔC_p vs. T plot (Figure 4), there exist two subsidiary small peaks at 312 and 346 K in addition to the main peak at 328 K. Before these small peaks are discussed, a few remarks on the experimental situation are in order. A fairly large amount of biferrocenium triiodide (10.9428 g) was used, however, as the relative atomic mass of iodine is extremely large compared to that of the other constituent atoms the iodine content in biferrocenium triiodide is as much as 50.7 wt%. For this reason, 10 g of biferrocenium triiodide is equivalent from the calorimetric point of view of ~6 g or less of some other compound that contains no heavy atoms. This "effectively small" amount of the present specimen represents a very unfavorable ratio of the heat capacity of the full calorimeter to that of the empty calorimeter. As a result, the heat capacity of the sample accounted for only 15% of the observed value for the full calorimeter at 100 K, 17% at 200 K, and 22% at 300 K. The present work, therefore, represents a test of the accuracy of the calorimeter.

As can be seen in Figure 4, this phase transition shows two characteristic features: one is a long ΔC_p tail extending to the low-temperature side, and the other is the presence of a few subsidiary ΔC_p peaks at 312 and 346 K. As to the first characteristic, the present ΔC_p vs. T curve shows recognizable deviation from the base line at ~220 K. This temperature is in good agreement with the temperature, ~215 K, at which the plot of the natural logarithm of the Mössbauer spectral area vs. temperature shows a "break" in a straight-line dependence.[15] It can be concluded that the intramolecular electron transfer begins to occur at ~220 K.

As to the presence of the subsidiary ΔC_p peaks, it is likely that these peaks are caused by the coexistence of samples with different histories. The ~11 g of biferrocenium triiodide sample used in the heat capacity experiments was prepared in two batches. It was our intention to prepare the sample in one reaction, but only 8.0 g were obtained in the first preparation, and thus a second batch of 3.4 g was prepared. Both batches were prepared in exactly the same manner and gave good chemical analyses. When the heat capacity measurements were being carried out, we expected that the two batches of the samples would show identical temperature dependencies of the rate of intramolecular electron-transfer behavior because they were prepared under the same experimental conditions. After the completion of the C_p measurements, however, we found that for certain mixed-valence biferrocenes, such as *1',6'-dibenzylbiferrocenium triiodide*,[15,16,19] the level of crystallinity of the compound dramatically affects the appearance of the Mössbauer spectrum (vide supra). It was proposed that the level of defect structure can vary from a microcrystalline to a diffusion-grown crystalline sample, and this can dramatically affect a cooperative phase transition.[15,16,19]

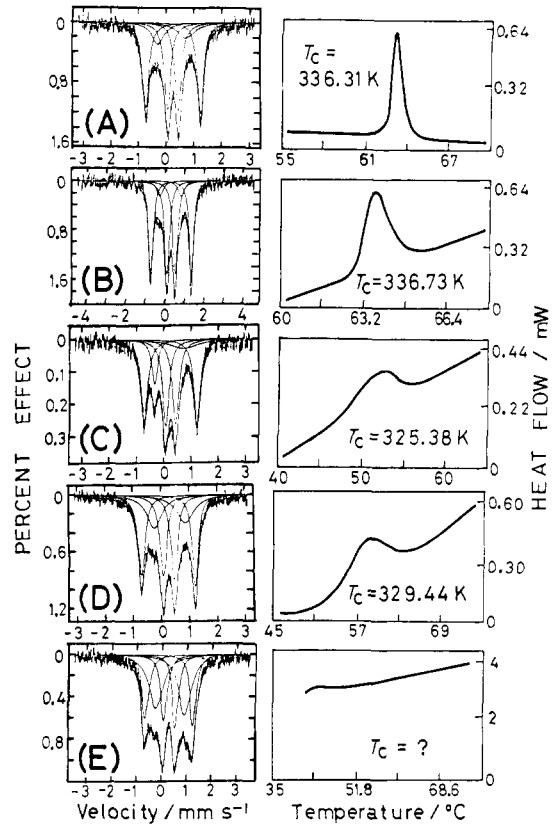

Figure 5. Sample history dependence of the ^{57}Fe Mössbauer spectrum at 300 K and DSC thermogram for biferrocenium triiodide. Samples A and B are two different microcrystalline samples that were prepared in the same manner. Sample C is comprised of recrystallized well-grown crystals. Samples D and E correspond to specimens taken from the two batches used for the heat capacity measurement. The DSC thermograms were run at a scan rate of 10 deg/min.

Table III. ^{57}Fe Mössbauer Spectra Recorded at 300 K for Biferrocenium Triiodide Crystals Prepared by Different Methods and Their DSC Thermograms

sample	Area fraction of the quadrupole-split doublets: electron localized, %	Area fraction of the quadrupole-split doublets: electron delocalized, %	peak temperature of DSC thermogram T_c, K
A	87.0	13.0	336.31
B	88.0	12.0	336.73
C	74.0	26.0	325.38
D	69.6	30.4	329.44
E	53.4	46.6	

On the other hand, in the case of the present biferrocenium triiodide, a similar sample history dependence of Mössbauer spectra was very recently found,[15] although the change in Mössbauer spectrum from one sample to another was not found to be so dramatic. In view of this sample history dependence we felt that it was important to examine simultaneously the Mössbauer spectrum and DSC thermogram for a number of different samples of biferrocenium triiodide. Figure 5 illustrates the ^{57}Fe Mössbauer spectra recorded at 300 K and DSC thermograms for various samples of *biferrocenium triiodide*. Each Mössbauer spectrum was least-squares fit to three quadrupole-split doublets. Two of the doublets correspond to a valence-trapped pattern; the areas of these two doublets were kept equal. The third doublet corresponds to the valence-detrapped species. In Table III are given the Mössbauer fitting parameters, which include the relative amounts of valence-trapped and valence-detrapped species, together with the peak temperature, T_c, obtained for each sample from a DSC thermogram. Samples A and B (of Table III) are two different microcrystalline samples which were prepared by slow (minutes) addition of an iodine/benzene solution to a benzene

solution of biferrocene. Both of these samples gave substantially the same 300 K Mössbauer spectrum: ~87.5% of a valence-trapped two-doublet pattern and ~12.5% of a valence-detrapped third doublet. The peak temperatures in the DSC thermograms were also found to be the same for samples A and B: T_c = 336.31 K for sample A and 336.73 K for sample B. It should be remarked, however, that the sharpness of the DSC peak is considerably different between samples A and B. Sample C was prepared by dissolving a microcrystalline sample in CH_2Cl_2 solution. After a period of time (0.5–1 day), crystals were formed by diffusing hexane slowly into the CH_2Cl_2 solution. This sample gave a 300 K Mössbauer spectrum with 74% of a valence-trapped two-doublet pattern and 26% of a valence-detrapped doublet. The DSC thermogram of sample C showed an endothermic peak that was broader than those observed for samples A and B. The peak temperature (T_c = 325.38 K) for this recrystallized sample was found to be lower than those observed for samples A and B. Samples D and E correspond to the 8.0-g and the 3.4-g portions, respectively, of biferrocenium triiodide which were combined to obtain the heat capacity sample. Fitting the 300 K Mössbauer spectrum for sample D indicated that there is 69.6% of a valence-trapped fraction and 30.4% of a valence-detrapped fraction. It can be seen in Figure 5 that the DSC thermogram of sample D shows an endothermic peak at 329.44 K that is also very broad. The most surprising results were obtained for sample E (the 3.4-g heat capacity batch). Fitting the 300 K Mössbauer spectrum for sample E indicates the presence of 53.4% of a valence-trapped fraction and 46.6% of a valence-detrapped fraction. This sample E has the largest amount of valence-detrapped signal that we have seen to date. It was surprising to find the DSC thermogram for sample E did not show a peak at temperatures above 315 K.

From these studies it is clear that there is a sample history dependence to the DSC peak. It seems that the DSC peak can even become so broad that it is difficult to see above the background of the DSC thermogram. In other words, the DSC endothermic peak of biferrocenium triiodide is sharper for a microcrystalline sample than for a diffusion-recrystallized sample, and the peak temperature is higher for the former than for the latter. This behavior is, however, unusual in comparison with usual magnetic phase transitions in which the heat capacity peak becomes broader and the peak temperature is displaced to lower temperature when the grain size is decreased.[40-42] It is clear from the above study of the sample history dependence of biferrocenium triiodide that there is no simple relationship between the manner in which the sample was prepared and the Mössbauer and DSC characteristics. The average crystal size in the case of the diffusion-grown sample C is larger than that of the samples obtained directly as microcrystals. However, certain microcrystalline samples (D and E) obviously exhibit DSC thermal effects as broad or even broader as sample C. It is likely that it is the variation in defect concentration from one sample to another which leads to the variation in Mössbauer and DSC characteristics. Obviously, it is difficult to determine the defect concentration for any sample.

With reference to the present heat capacity measurements, the main heat capacity peak at 328 K (see Figure 4) can be attributed to a phase-transition characteristic of sample D, while the peak at 312 K would be due to sample E. The origin of the peak at 346 K could also be intramolecular electron transfer in microcrystallites with different defect concentrations which might be contained in samples D and E. At any rate, it is evident that biferrocenium triiodide crystals are in the valence-trapped state at low temperatures and in the valence-detrapped state above 350 K independent of crystal sizes and defect concentrations. Therefore, as far as we are concerned not with the heat capacity curve itself but with the transition entropy, there is no problem even if the present calorimetric specimen consists of a mixture of two batches of crystallites with different sample histories.

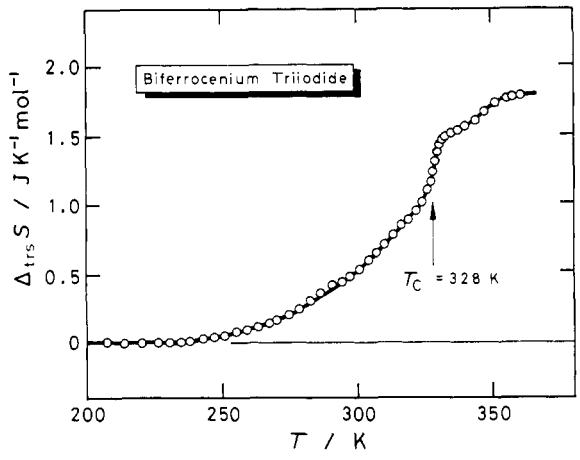

Figure 6. Temperature dependence of the transition entropy of biferrocenium triiodide.

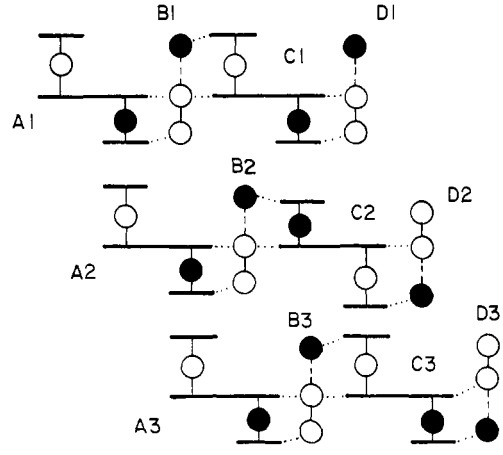

Figure 7. Schematic representation of the packing arrangement of mixed-valence cations and trihalide anions in biferrocenium triiodide. The dotted lines indicate possible hydrogen-bonding contacts.

Nature of and Entropy Change Associated with Phase Transition. The temperature dependence of the transition entropy is shown in Figure 6. At the outset it should be commented that the entropy acquisition, ΔS_{trs} = (1.77 ± 0.06) J K^{-1} mol^{-1}, is unexpectedly small even if we take into account only the contribution from the mixed-valence binuclear cations converting from valence trapped to valence detrapped, which amounts to R ln 2 (=5.76 J K^{-1} mol^{-1}) where R is the gas constant. It is appropriate at this point to give a qualitative description of the likely microscopic nature of the phase transition observed for biferrocenium triiodide. A schematic view of the packing arrangement in this compound is shown in Figure 7. In this figure each mixed-valence biferrocenium cation is schematically represented as

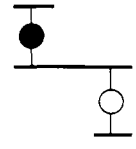

The Fe^{III} ion is indicated with an open circle. The cations are stacked in a stepwise fashion with four stacks of anions about each cation stack.[15,16] Part of two stacks of cations are indicated in Figure 7. The intercation interactions are appreciable with intermolecular cp···cp interplanar distances of 3.4 Å.

A binuclear mixed-valence biferrocenium cation has two electronic states, [$Fe_A^{II}Fe_B^{III}$] and [$Fe_A^{III}Fe_B^{II}$], which are coupled to an out-of-phase combination of symmetric cp–Fe–cp stretching modes, one on each metallocene unit. An intramolecular electronic interaction induces the electron transfer between the two vibronic states of a double-well potential energy diagram. During this transfer the dimensions of the Fe^{III} metallocene become smaller

(40) Fisher, M. E.; Ferdinand, A. E. *Phys. Rev. Lett.* **1967**, *19*, 169.
(41) Ferdinand, A. E.; Fisher, M. E. *Phys. Rev.* **1969**, *185*, 832.
(42) Sorai, M.; Kosaki, A.; Suga, H.; Seki, S. *J. Chem. Thermodyn.* **1969**, *1*, 119.

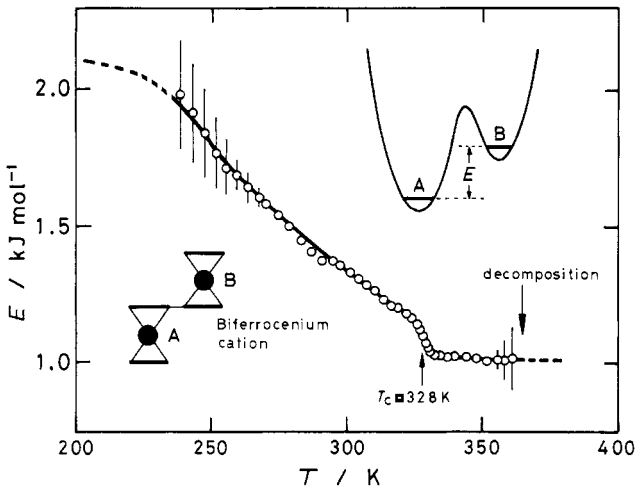

Figure 8. Temperature dependence of the potential energy difference, E, between the two vibronic states in the mixed-valence biferrocenium cation, $[Fe_A^{II}Fe_B^{III}]$ and $[Fe_A^{III}Fe_B^{II}]$. The inset shows the potential energy curve for the ground state of such a mixed-valence complex.

and those of the Fe^{III} metallocene larger. As is obvious from Figure 7, each biferrocenium cation cannot transfer an electron independently of its neighboring cations in the same stack. The transferring of electrons has to occur cooperatively in a given stack. Thus, not only is the magnitude of the potential energy barrier for electron transfer in an individual cation important, but the intercation interaction can also be rate determining if it is of the appropriate magnitude. In fact, the presence of this intercation interaction leads to a valence localization at low temperatures by introducing a zero-point energy difference between the two vibronic states of a cation; that is, it stabilizes the valence-localized state.

In order to have a phase transition involving intramolecular electron transfer in biferrocenium triiodide, it is necessary to have intermolecular interactions develop in more than one dimension (i.e., only along one stack). In recent articles we have shown[16-18] that by simply changing the anion from I_3^- to Br_2I^-, for example, there can be dramatic changes in the rate of intramolecular electron transfer in the mixed-valence cation. It seems reasonable then to suggest that cation–anion interactions are important, as well as cation–cation interactions. The exact nature of the cation–anion interaction is not clear. In the case of trihalide anions we have suggested[16-18] two possibilities. On the one hand, the I_3^- ion, for example, could be oscillating between two distorted states, $I_A^-\cdots I_B-I_C$ and $I_A-I_B\cdots I_C^-$ in the extreme case. This charge oscillation in the I_3^- anion could couple to the electron transfer in the mixed-valence cation. On the other hand, the whole I_3^- anion could at some temperature begin to move between two nearby lattice positions. This second type of charge oscillation associated with the I_3^- anions would have the same effect as the other type of charge oscillation. As we have shown in a theoretical model,[43] the net result of this interaction of the cation with its neighboring I_3^- anions is to lead to a cooperativity between cation stacks. With intermolecular interactions developing in three dimensions it is possible to have a phase transition. A simple question arises as to why the entropy change due to the phase transition is so small. One possible explanation for the small value of ΔS_{trs} is that the zero-point energy difference (E) between the two minima in the double-well potential energy curve is temperature dependent (see inset in Figure 8). If the two vibronic states $[Fe_A^{II}Fe_B^{III}]$ and $[Fe_A^{III}Fe_B^{II}]$ are of the same energy ($E = 0$, see inset in Figure 8), then the transformation from electronically localized to delocalized would give $\Delta S_{trs} = R \ln 2$. If E is temperature dependent, decreasing in value with increasing temperature, this could explain the small value of ΔS_{trs}. The entropy due to this energy scheme is given by eq 2, where Z is the partition function.

$$S = R \ln Z + (E/ZT) \exp(-E/RT) \quad (2)$$

$$Z = 1 + \exp(-E/RT) \quad (3)$$

When the left-hand side of eq 2 is replaced by the tranition entropy at a given temperature T, $\Delta S_{trs}(T)$, one can obtain the temperature dependence of the energy difference, $E(T)$. The results are shown in Figure 8. The value of $E(T)$ at 200 K was found to be $\sim$2.1 kJ mol^{-1}, which corresponds to 253 K in terms of thermal energy. When the transition temperature, T_c = 328 K, is approached, the value of $E(T)$ gradually decreases to $\sim$1.0 kJ mol^{-1} (120 K in terms of thermal energy). Above T_c, the value of $E(T)$ remains constant. If the phase transition occurs completely, the energy difference $E(T)$ should be zero at T_c in a mean-field approximation. Therefore, the phase transition in biferrocenium triiodide appears to be incomplete. In other words, the "extra" electron favorably stays on one Fe ion for longer periods than on the other Fe ion even above the phase-transition point.

There is another possible explanation for the small value of ΔS_{trs} observed for the phase transition of biferrocenium triiodide compared to the theoretical expectation of $\Delta S = R \ln 2$. This second possibility can be made clear by reference to papers in which the order–disorder phase transition observed for mixed-valence Eu_3S_4 has been characterized. Early X-ray diffraction results[44,45] suggested that Eu_3S_4 undergoes a structural transformation at 160 K, such that above this temperature all Eu ions are equivalent whereas, below 160 K the valences become trapped to give $Eu^{II}Eu_2^{III}S_4$. However, these X-ray results did not definitively substantiate this model. In support of the model, Berkooz et al.[46] have interpreted the temperature dependence of the ^{151}Eu Mössbauer spectrum between 83 K and room temperature in terms of thermally activated electron hopping among the Eu sites. If there is an order–disorder phase transition for Eu_3S_4 where the compound becomes electronically delocalized above the phase-transition temperature, then an entropy increase of $\Delta S = R \ln 3$ (=9.13 J K^{-1} mol^{-1}) would be expected.[47] It was puzzling then that an experimental determination[48] of ΔS gave 3.3 J K^{-1} for a *microcrystalline* sample of Eu_3S_4. Massenet, Coey, and Holtzberg[48] speculated that the small value of the experimental ΔS "suggests that there remains a large amount of short range order in the distribution of europium valencies above the transition". Very recently, Pott et al.[49] carried out heat capacity measurements for a 0.4932-g *single crystal* of Eu_3S_4. They found a first-order phase transition at 186 K with $\Delta S = 9 \pm 0.9$ J K^{-1}, which agrees with the theoretical expectation of $R \ln 3$. Pott et al.[49] also demonsrated with capacitive thermal expansion and electrical resistivity measurements that Eu_3S_4 undergoes a first-order, nonstructural phase transition at 186 K. They attributed the difference in ΔS value obtained for a single crystal of Eu_3S_4 compared to that obtained for a microcrystalline sample to the "better sample quality" of the single crystal.

Thus, the small value of ΔS_{trs} observed for the biferrocenium triiodide phase transition could be attributable to poor crystal quality associated with the small crystals in the microcrystalline sample. It would be expected that if a relatively large single crystal could be obtained, then the experimental ΔS_{trs} value would approach closer to the $R \ln 2$ theoretical expectation. The small crystals in the microcrystalline sample could have a high concentration of imperfections such as dislocations, cluster defects, or grain boundaries. Such imperfections influence the kinetics of phase transitions.[50] Defects function in a duality of roles. They

(43) Kambara, T.; Hendrickson, D. N.; Dong, T.-Y.; Cohn, M. J. *J. Chem. Phys.* **1987**, *86*, 2362.

(44) Bransky, I.; Tallan, N. M.; Hed, A. Z. *J. Appl. Phys.* **1970**, *41*, 1187.

(45) Davis, H. H.; Bransky, I.; Tallan, N. M. *J. Less-Common Met.* **1970**, *22*, 193.

(46) Berkooz, O.; Lalamud, M.; Shtrikmann, S. *Solid State Commun.* **1968**, *6*, 185.

(47) For general discussions of charge ordering at low temperatures, see: (a) Mott, N. F. *Philos. Mag.*, [*Part*] *B* **1980**, *B42*, 325. (b) Holtzberg, F. *Philos. Mag.* [*Part*] *B* **1980**, *B42*, 491.

(48) Massenet, O.; Coey, J. M. D.; Holtzberg, F. *J. Phys.* (*Paris*) *Colloq.* **1976**, *37*, C4-297.

(49) Pott, R.; Güntherodt, G.; Wichelhaus, W.; Ohl, M.; Bach, H. *Phys. Rev. B.* **1983**, *27*, 359.

serve as preferred sites for nucleation of the minority phase in the presence of the majority phase. On the other hand, when a critical-size nucleus of the minority phase impinges upon a defect as it is growing, this increases the activation energy for further growth of the minority-phase nucleus. It is possible, then, that appreciable defect concentration in a microcrystalline sample could lead to the phase transition for some part of the sample to occur over such a large temperature range that it is virtually impossible to discern the thermal effect associated with this fraction of the sample above the background of the normal heat capacity of the lattice. It must be emphasized that this problem of "poor crystal quality" is probably a general problem, not just a phenomenon characteristic of a few systems.

Role of the I_3^- Anion in the Phase Transition. For the rate of intramolecular electron transfer in mixed-valence biferrocenes, an important role of the trihalide counteranions has been recognized.[16-18] For example, the change from I_3^- in biferrocenium triiodide to Br_2I^- leads to a change of ~150 K in the temperature at which the mixed-valence biferrocenium cations transfer electrons faster than the Mössbauer time scale.[16,17] In the case of 1',6'-diiodobiferrocenium trihalides, the I_3^- salt shows Mössbauer spectra characteristic of a valence-detrapped state between 4.2 and 300 K,[22] while the Br_2I^- salt is in a valence-trapped state at 4.2 K and its Mössbauer spectrum changes to become eventually a single average-valence doublet above 80 K.[18] Similar behavior has been observed between the I_3^- and Br_2I^- salts of 1',6'-dibromobiferrocene.[18]

It is appropriate then to examine whether or not such a charge oscillation in I_3^- anions really occurs in biferrocenium triiodide to an extent that it influences the rate of intramolecular electron transfer in the biferrocenium cations. To this end, structural analysis by X-ray (or neutron) diffraction and spectroscopies such as IR and Raman are complementarily useful. A merit of the former method is to provide accurate bond lengths and bond angles, whereas the information is often of a spatial- and time-averaged type. On the other hand, vibrational spectroscopic methods can afford instantaneous structural information detected on the time scale of lattice vibrations ($\sim 10^{-13}$ s). Three of the present authors and their collaborators[15,16] have already reported the single-crystal X-ray structure of biferrocenium triiodide at 296 K. According to these results, the space group is $P\bar{1}$ and both the cation and the anion sit on centers of symmetry. The I_3^- anion is centrosymmetric with a bond length of 2.9292 Å. As far as this structural work is concerned, the charge oscillation does not seem to exist in the I_3^- ion. However, the 300 K Mössbauer spectrum of this compound always shows the presence of an appreciable amount of valence-trapped cations in spite of the fact the X-ray work indicates a centrosymmetric structure for the mixed-valence biferrocenium cation. This conflict seems to arise from the statistical nature inherent in X-ray diffraction. It was important to investigate the structure of I_3^- anion from the spectroscopic viewpoint.

A linear, symmetric triatomic ion such as I_3^- has three fundamental modes of vibration: the symmetric stretching mode (ν_1), the doubly degenerate deformation mode (ν_2), and the asymmetric stretching mode (ν_3). The ν_1 mode is Raman active and IR inactive, while the ν_2 and ν_3 modes are exclusively IR active. In the condensed phase, distortion of the I_3^- ion from a linear symmetrical structure allows all three modes to show both IR and Raman activity. The distorted ion can have either an unsymmetrical linear form or a nonlinear form. Therefore, examination of the intensity in the IR and Raman spectra of the ν_1, ν_2, and ν_3 bands of the I_3^- ion has a diagnostic value for determination of the I_3^- structure in biferrocenium triiodide.

Since the ν_1, ν_2, and ν_3 modes appear, if active, below 200 cm^{-1}, IR and Raman spectra for biferrocenium triiodide were carefully recorded in the ranges 400–30 cm^{-1} and 300–40 cm^{-1}, respectively. IR spectra for biferrocenium triiodide at 340, 299, and 101 K are reproduced in Figure 9. Also shown in this figure for comparison

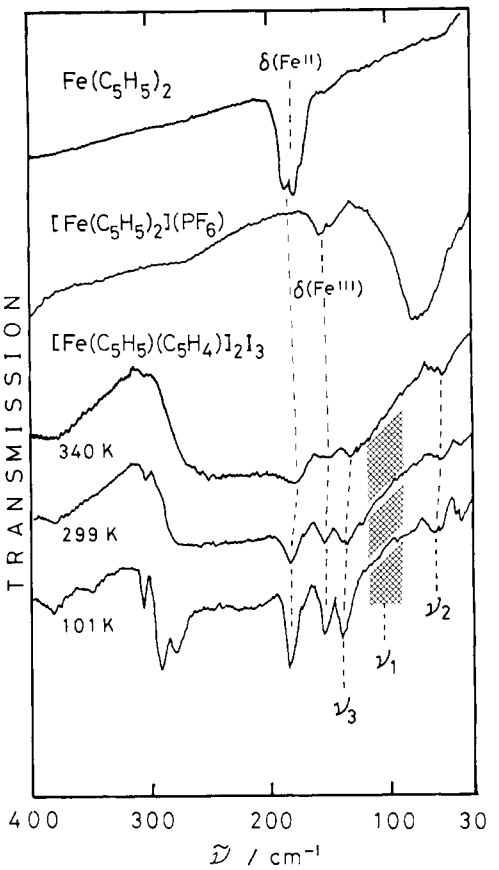

Figure 9. Far-infrared absorption spectra for biferrocenium triiodide, ferrocene, and ferrocenium hexafluorophosphate[44] in the range 400–30 cm^{-1}. ν_2 and ν_3 indicate the deformation and asymmetric stretching modes of I_3^- ion. The shaded area corresponds to the wavenumber region for the symmetric stretching ν_1 mode that would appear if I_3^- ion has a nonlinear form or an unsymmetrical linear form. $\delta(Fe^{II})$ and $\delta(Fe^{III})$ are the ring–metal–ring bending modes for ferrocene and ferrocenium cation, respectively.

are IR spectra for ferrocene and ferrocenium hexafluorophosphate.[51] The IR absorption bands observed for biferrocenium triiodide below 200 cm^{-1} at 299 K were located at 55, 136, 153, and 183 cm^{-1}. Except for a slight frequency shift with temperature, these four bands are observed in both the 101 and 340 K spectra. Since ferrocene crystal[52,53] exhibits the doubly degenerate ring–metal–ring bending mode, $\delta(Fe^{II})$, as a doublet at 187/178 cm^{-1}, the 183-cm^{-1} band can be assigned to this mode of the ferrocene moiety in the biferrocenium cation. Similarly, the 153-cm^{-1} band may be assigned to the ring–metal–ring bending mode of the ferrocenium moiety $\delta(Fe^{III})$, because ferrocenium hexafluorophosphate shows this band at 156/147 cm^{-1}. For the reason described below, the 55- and 136-cm^{-1} bands can be assigned to the ν_2 and ν_3 modes of the I_3^- ion.

Laser Raman spectra of biferrocenium triiodide were recorded by using the 632.8-nm line from a He–Ne source for excitation and the 514.5-nm line from an Ar source (see Figure 10). At 295 K a strong band is seen at 111 and 110 cm^{-1} for the He–Ne and Ar sources, respectively. This band can be assigned to the ν_1 mode of I_3^- ion for the reason given below.

Table IV lists the bond lengths and angles asociated with I_3^-/ion and with the ν_1, ν_2, and ν_3 frequencies in those compounds for

(50) Rao, C. N. R.; Rao, K. J. *Phase Transitions in Solids*; McGraw-Hill: New York, 1978.
(51) Shiomi, Y.; Sorai, M., manuscript in preparation.
(52) Lippincott, E. R. Nelson, R. D. *Spectrochim. Acta* **1958**, *10*, 307.
(53) Sorai, M.; Shiomi, Y. *Mol. Cryst. Liq. Cryst.* **1984**, *107*, 271.
(54) Hayward, G. C.; Hendra, P. J. *Spectrochim. Acta, Part A* **1967**, *23A*, 2309.
(55) Teitelbaum, R. C.; Ruby, S. L.; Marks, T. J. *J. Am. Chem. Soc.* **1979**, *101*, 7568.
(56) Havinga, E. E.; Boswijk, K. H.; Wiebenga, E. H. *Acta Crystallogr.* **1954**, *7*, 487.
(57) Mooney, R. C. *Phys. Rev.* **1938**, *53*, 851.

Table IV. Geometry of I_3^- Ion and Normal Modes of Vibration in the Solid State at Room Temperature[a]

compd	$R(I_A-I_B)$, Å	$R(I_B-I_C)$, Å	$R(I_A-I_C)$, Å	$I_AI_BI_C$, deg	ν_1, cm^{-1}	ν_2, cm^{-1}	ν_3, cm^{-1}	remark	ref X-ray	ref IR or Raman
CsI_3	2.840	3.042	5.882	177.9	103	69	149	IR (>50 cm^{-1})	38	37
							150	IR (>70 cm^{-1})		54
					99		146	Raman (>70 cm^{-1})		55
Cs_2I_8	2.85	3.00	5.85	176.8	105		150	Raman (>70 cm^{-1})	56	55
$(C_6H_5)_4AsI_3$	2.920	2.920	5.840	175.61	113			Raman (>70 cm^{-1})	38	55
$(CH_3)_4NI_3$	2.75	2.75	5.50	180			143	IR (>70 cm^{-1})	57	54
					111		143	Raman (nitrobenzene)		37
					109		152	Raman (ethanol)		37
biferrocenium triiodide	2.9292	2.9292	5.8584	180.0	no	55	136	IR (>30 cm^{-1})	15	present work
					110	no	no	Raman (>40 cm^{-1})		present work

[a] Modes of vibration: ν_1, symmetric stretching mode; ν_2, deformation; ν_3, asymmetric stretching mode. Raman data of $(CH_3)_4NI_3$ in nitrobenzene and ethanol solutions are also included for comparison.

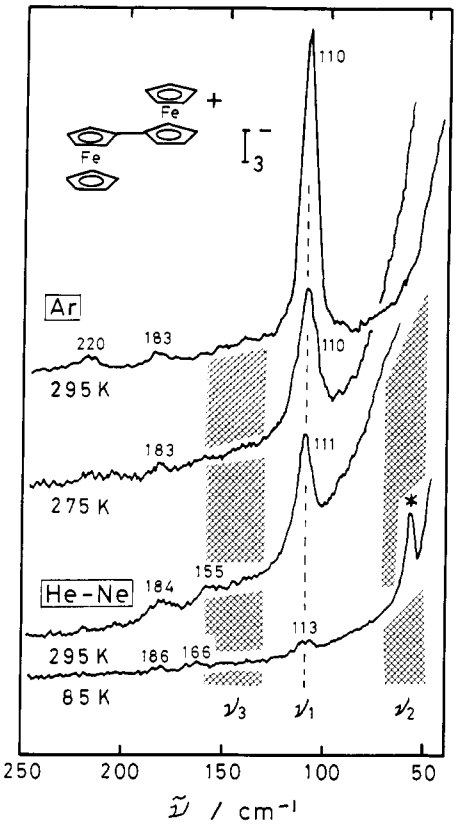

Figure 10. Laser Raman spectra of biferrocenium triiodide in the range 250–40 cm^{-1}, recorded by using a He–Ne and an Ar source. ν_1 is the symmetric stretching mode of I_3^- ion. Two shaded areas correspond to the wavenumber regions for the deformation and asymmetric stretching modes of I_3^- ion that would appear if I_3^- ion has a nonlinear form or an unsymmetrical linear form. The peak indicated with an asterisk is due to the natural emission from the He–Ne laser.

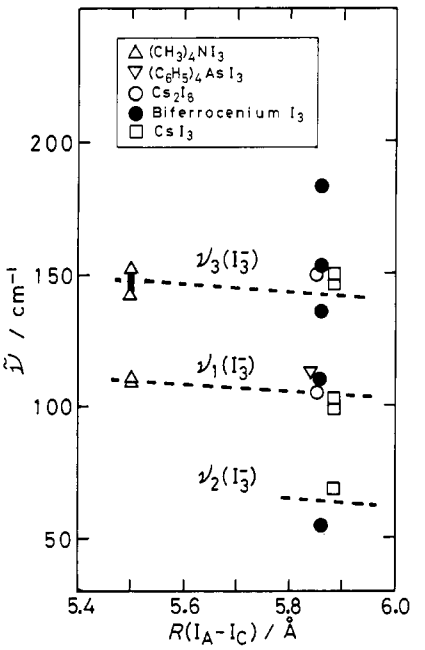

Figure 11. Dependence of the ν_1, ν_2, and ν_3 fundamental modes of vibration in I_3^- ion upon the bond length between the two terminal atoms of the I_3^- anion for various compounds. For biferrocenium triiodide, all the bands observed in IR and Raman spectra below 200 cm^{-1} are plotted.

which both structural and spectroscopic data at room temperature are available. In order to estimate the wavenumbers expected for the ν_1, ν_2, and ν_3 modes of biferrocenium triiodide, the IR and Raman data given in Table IV have been plotted in Figure 11 as a function of the distance between the two terminal atoms of the triiodide anion, $R(I_A-I_C)$. Although the available data are limited, the wavenumbers of the three fundamental modes characteristic of the I_3^- ion seem to change linearly with the bond length at least in the narrow range of $R(I_A-I_C)$ shown in Figure 11. As is evident in Figure 11, the Raman peak at 110 cm^{-1} observed for biferrocenium triiodide is located very near the ν_1 line, while the 55- and 136-cm^{-1} bands recorded in the IR spectra are located near the ν_2 and ν_3 lines, respectively. Based on this fact, we assign the 110-, 55-, and 136-cm^{-1} bands observed for biferrocenium triiodide to the ν_1, ν_2, and ν_3 modes of the I_3^- anion, respectively.

As seen in Table IV, the mutual exclusion rule has broken down when the I_3^- ion is nonlinear. Shaded areas in Figures 9 and 10 represent the wavenumber regions in which the fundamental modes of the I_3^- anion might appear when the I_3^- anion is unsymmetrical or nonlinear. Within the resolutions of the present spectrophotometers, the ν_1 band is not seen in the IR spectrum and the ν_2 and ν_3 bands are not seen in the Raman spectrum. Therefore, it is possible to conclude that the I_3^- anion in biferrocenium triiodide is not very unsymmetrical even at 101 K.

As an additional check on the IR and Raman probing of the structure of the I_3^- anion, we decided to determine what is seen for 1′,6′-dichlorobiferrocenium triiodide hemiiodine, the $0.5I_2$ solvate of compound **2**. The single-crystal X-ray structure of this compound was reported[14] recently. In this compound the I_3^- anion sits closer to the Fe^{III} metallocene moiety than the Fe^{II} metallocene moiety of the neighboring mixed-valence cation. As a result, the cation is valence trapped even at 340 K. Furthermore, the I_3^- anion is unsymmetric with I–I bond lengths of 2.848 (6) and 3.00 (6) Å. Examination of the far-IR and Raman spectra for this compound, as illustrated in Figures 12 and 13, respectively, shows that the ν_1, ν_2, and ν_3 bands of the I_3^- anion are seen in both the IR and Raman spectra. At 97 K the IR spectrum exhibits the ν_1, ν_2, and ν_3 bands at 106, 66, and 142 cm^{-1}, respectively. A comparison with the IR spectrum of biferrocenium triiodide in Figure 9 shows that the intensity of the ν_1 band for this $2.5I_2$ compound is quite appreciable.

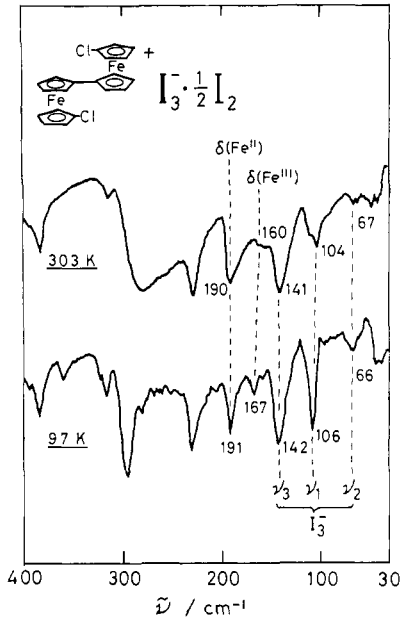

Figure 12. Far-infrared absorption spectra for 1′,6′-dichlorobiferrocenium triiodide hemiiodine in the range 400–30 cm^{-1}. ν_1, ν_2, and ν_3 indicate the symmetric stretching, deformation, and asymmetric stretching modes of the I_3^- anion. δ(Fe^{II}) and δ(Fe^{III}) are the ring–metal–ring bending modes for the Fe^{II} and Fe^{III} metallocene moieties, respectively.

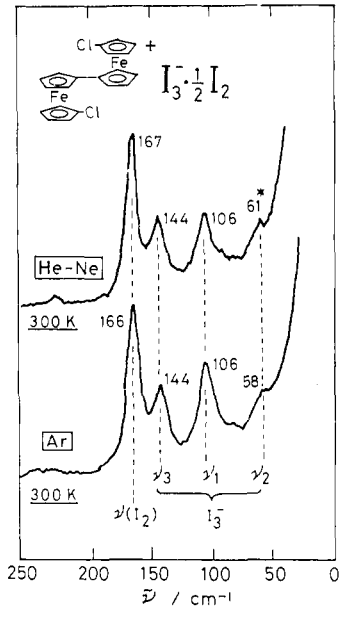

Figure 13. Laser Raman spectra of 1′,6′-dichlorobiferrocenium triiodide hemiiodine in the range 250–40 cm^{-1}, recorded by using either a He–Ne or an Ar source. See the caption for Figure 12 for a definition of ν_1, ν_2, and ν_3.

The above comparison brings to mind a question: just how intense would the ν_1 band be expected to be in the IR spectrum of biferrocenium triiodide if the I_3^- anion did become only slightly unsymmetric? That is, in a valence-trapped mixed-valence biferrocenium cation it is known[14] that the centroid-to-centroid cp–cp (ring-to-ring) distances of the Fe^{II} and Fe^{III} metallocenes only differ by ~0.08 Å. If the I_3^- anion is sitting next to such a mixed-valence cation oriented such that the I–I–I direction is perpendicular to the fulvalenide ligand, then the I–I bond lengths might only differ by 0.08 Å or even less. Obviously, this is a considerably smaller difference in bond lengths than what is observed for the I_3^- anion in $2.5I_2$[14] and other structurally characterized valence-trapped mixed-valence biferrocenes.[20,58] It would be interesting to know if the ν_1 band would show much intensity in the IR spectrum for an I_3^- salt which has a small amount of I–I bond length asymmetry.

Conclusions and Comments

A higher order phase transition which starts at ~220 K and with the main C_p peak at 328 K has been found for mixed-valence biferrocenium triiodide in heat capacity measurements. In this same temperature region the ^{57}Fe Mössbauer spectrum does change from a valence-trapped two-doublet pattern to a valence-detrapped single-doublet pattern. There is a sample history dependence in the appearance of both the thermal effect in the DSC thermogram and the Mössbauer spectrum at 300 K. Samples which show more valence-detrapped signal in the 300 K Mössbauer spectrum have broader peaks in the DSC thermogram. The entropy of acquisition, $\Delta S_{trs} = (1.77 \pm 0.06)$ J K^{-1} mol^{-1}, for the phase transition falls considerably short of a simple R ln 2 (=5.76 J K^{-1} mol^{-1}) expectation for the biferrocenium cation converting from valence trapped to valence detrapped. The possibility that the I_3^- anion in biferrocenium triiodide converts from unsymmetric at low temperatures to dynamically symmetric at high temperatures has been examined with far-infrared and Raman data. The absence of much intensity associated with the symmetric (ν_1) stretching I_3^- band in the IR spectrum indicates that I_3^- does *not* become very unsymmetric even at low temperatures.

A qualitative description of the microscopic nature of the phase transition observed for biferrocenium triiodide has been presented. A quantitative model is available.[43] It is clear there are important intermolecular interactions between mixed-valence cations in the stepwise stacks of cations. The exact influence and role of the I_3^- counteranions in the phase transition has not been totally elucidated. The onset of charge oscillation with the I–I–I$^-$ array or the onset of movement of the whole I_3^- anion has been suggested as a possibility for the manner in which three-dimensional cooperativity develops. It is clear that further study of this and the sample history dependence is needed.

Acknowledgment. We are grateful for valuable discussions with Professors H. Sano (Tokyo Metropolitan University), M. Kobayashi (Osaka University), and T. Kambara (the University of Electro-Communications, Tokyo) and for the recording of IR and Raman spectra by S. Ishikawa, T. Yamamoto, and M. Ohama. The research at the University of Illinois was funded in part by National Institutes of Health Grant HL13652. One of the authors (M.S.) is grateful for funding from the Ministry of Education, Science, and Culture in the form of a Grant-in-Aid for Scientific Research 61540325.

(58) Kramer, J. A.; Herbstein, F. H.; Hendrickson, D. N. *J. Am. Chem. Soc.* **1980**, *102*, 2293.